Attosecond emission from chromium plasma

L Elouga Bom, Stefan Haessler, O Gobert, M Perdrix, F Lepetit, J.-F Hergott, B Carré, T Ozaki, Pascal Salières

Attosecond emission from chromium plasma

L. B. Elouga Bom,[1] S. Haessler,[2,3] O. Gobert,[2] M. Perdrix,[2] F. Lepetit,[2] J.-F. Hergott,[2] B. Carré,[2] T. Ozaki,[1] and P. Salières[2,*]

[1]*Institut national de la recherche scientifique – Centre Energie, Matériaux et Télécommunications, 1650 Lionel-Boulet, Varennes, Québec J3X 1S2, Canada*
[2]*IRAMIS-Service des Photons, Atomes et Molécules, CEA Saclay, 91191 Gif-sur-Yvette Cedex, France*
[3]*Photonics Institute, Vienna University of Technology, Gusshausstrasse 27/387, A-1040 Vienna, Austria*
[*]*pascal.salieres@cea.fr*

Abstract: We present the first measurement of the attosecond emission generated from underdense plasma produced on a solid target. We generate high-order harmonics of a femtosecond Ti:sapphire laser focused in a weakly ionized underdense chromium plasma. Using the "Reconstruction of Attosecond Beating by Interference of Two-photon Transitions" (RABITT) technique, we show that the 11^{th} to the 19^{th} harmonic orders form in the time domain an attosecond pulse train with each pulse having 300 as duration, which is only 1.05 times the theoretical Fourier transform limit. Measurements reveal a very low positive group delay dispersion of 4200 as^2. Beside its fundamental interest, high-order harmonic generation in plasma plumes could thus provide an intense source of attosecond pulses for applications.

OCIS codes: (190.0190) Nonlinear optics; (190.4160) Multiharmonic generation.

References and links

1. P. Antoine, A. L'Huillier, and M. Lewenstein, "Attosecond pulse trains using high-order harmonics," Phys. Rev. Lett. **77**, 1234–1237 (1996).
2. P. M. Paul, E. S. Toma, P. Breger, G. Mullot, F. Auge, P. Balcou, H. G. Muller, and P. Agostini, "Observation of a train of attosecond pulses from high harmonic generation," Science **292**, 1689–1692 (2001).
3. M. Hentschel, R. Kienberger, C. Spielmann, G. Reider, N. Milosevic, T. Brabec, P. Corkum, U. Heinzmann, M. Drescher, and F. Krausz, "Attosecond metrology," Nature **414**, 509–513 (2001).
4. P. Johnsson, R. López Martens, S. Kazamias, J. Mauritsson, C. Valentin, T. Remetter, K. Varjú, M. B. Gaarde, Y. Mairesse, H. Wabnitz, P. Salières, P. Balcou, K. J. Schafer, and A. L'Huillier, "Attosecond electron wave packet dynamics in strong laser fields," Phys. Rev. Lett. **95**, 013001 (2005).
5. J. Mauritsson, P. Johnsson, E. Mansten, M. Swoboda, T. Ruchon, A. L'Huillier, and K. Schafer, "Coherent electron scattering captured by an attosecond quantum stroboscope," Phys. Rev. Lett. **100**, 073003 (2008).
6. S. Haessler, B. Fabre, J. Higuet, J. Caillat, T. Ruchon, P. Breger, B. Carré, E. Constant, A. Maquet, E. Mével, P. Salières, R. Taïeb, and Y. Mairesse, "Phase-resolved attosecond near-threshold photoionization of molecular nitrogen," Phys. Rev. A **80**, 011404(R) (2009).
7. M. Drescher, M. Hentschel, R. Kienberger, M. Uiberacker, V. Yakovlev, A. Scrinzi, T. Westerwalbesloh, U. Kleineberg, U. Heinzmann, and F. Krausz, "Time-resolved atomic inner-shell spectroscopy," Nature **419**, 803–807 (2002).
8. A. Föhlisch, P. Feulner, F. Hennies, A. Fink, D. Menzel, D. Sanchez-Portal, P. M. Echenique, and W. Wurth, "Direct observation of electron dynamics in the attosecond domain," Nature **436**, 373–376 (2005).
9. A. Cavalieri, N. Muller, T. Uphues, V. Yakovlev, A. Baltuška, B. Horvath, B. Schmidt, L. Blumel, R. Holzwarth, S. Hendel, M. Drescher, U. Kleineberg, P. Echenique, R. Kienberger, F. Krausz, and U. Heinzmann, "Attosecond spectroscopy in condensed matter," Nature **449**, 1029–1032 (2007).

#139154 - $15.00 USD Received 3 Dec 2010; revised 17 Jan 2011; accepted 17 Jan 2011; published 10 Feb 2011

10. M. Uiberacker, T. Uphues, M. Schultze, A. Verhoef, V. Yakovlev, M. Kling, J. Rauschenberger, N. Kabachnik, H. Schroder, M. Lezius, K. Kompa, H. G. Muller, M. Vrakking, S. Hendel, U. Kleineberg, U. Heinzmann, M. Drescher, and F. Krausz, "Attosecond real-time observation of electron tunnelling in atoms," Nature **446**, 627–632 (2007).
11. W. Boutu, S. Haessler, H. Merdji, P. Breger, G. Waters, M. Stankiewicz, L. J. Frasinski, R. Taïeb, J. Caillat, A. Maquet, P. Monchicourt, B. Carré, and P. Salières, "Coherent control of attosecond emission from aligned molecules," Nat. Phys. **4**, 545–549 (2008).
12. J. Itatani, J. Levesque, D. Zeidler, H. Niikura, H. Pepin, J. C. Kieffer, P. B. Corkum, and D. M. Villeneuve, "Tomographic imaging of molecular orbitals," Nature **432**, 867–871 (2004).
13. S. Haessler, J. Caillat, W. Boutu, C. Giovanetti-Teixeira, T. Ruchon, T. Auguste, Z. Diveki, P. Breger, A. Maquet, B. Carre, R. Taïeb, and P. Salieres, "Attosecond imaging of molecular electronic wavepackets," Nat. Phys. **6**, 200–206 (2010).
14. E. A. Gibson, A. Paul, N. Wagner, R. Tobey, S. Backus, I. P. Christov, M. M. Murnane, and H. C. Kapteyn, "High-order harmonic generation up to 250 eV from highly ionized argon," Phys. Rev. Lett. **92**, 033001 (2004).
15. L. B. Elouga Bom, J. Kieffer, R. Ganeev, M. Suzuki, H. Kuroda, and T. Ozaki, "Influence of the main pulse and prepulse intensity on high-order harmonic generation in silver plasma ablation," Phys. Rev. A **75**, 033804–033808 (2007).
16. Y. Nomura, R. Hörlein, P. Tzallas, B. Dromey, S. Rykovanov, Z. Major, J. Osterhoff, S. Karsch, L. Veisz, M. Zepf, D. Charalambidis, F. Krausz, and G. D. Tsakiris, "Attosecond phase locking of harmonics emitted from laser-produced plasmas," Nat. Phys. **5**, 124–128 (2008).
17. Y. Akiyama, K. Midorikawa, Y. Matsunawa, Y. Nagata, M. Obara, H. Tashiro, and K. Toyoda, "Generation of high-order harmonics using laser-produced rare-gas-like ions," Phys. Rev. Lett. **69**, 2176–2179 (1992).
18. C. G. Wahlström, S. Borgström, J. Larsson, and S. G. Pettersson, "High-order harmonic generation in laser-produced ions using a near-infrared laser," Phys. Rev. A **51**, 585–591 (1995).
19. R. Ganeev, M. Baba, M. Suzuki, and H. Kuroda, "High-order harmonic generation from silver plasma," Phys. Lett. A **339**, 103–109 (2005).
20. J. F. Hergott, M. Kovacev, H. Merdji, C. Hubert, Y. Mairesse, E. Jean, P. Breger, P. Agostini, B. Carré, and P. Salières, "Extreme-ultraviolet high-order harmonic pulses in the microjoule range," Phys. Rev. A **66**, 021801 (2002).
21. R. Ganeev, Luc, T. Ozaki, and P. Redkin, "Maximizing the yield and cutoff of high-order harmonic generation from plasma plume," J. Opt. Soc. Am. B **24**, 2770–2778 (2007).
22. R. Ganeev, E. Bom, J. Kieffer, M. Suzuki, H. Kuroda, and T. Ozaki, "Demonstration of the 101st harmonic generated from a laser-produced manganese plasma," Phys. Rev. A **76**, 023831–023837 (2007).
23. R. Ganeev, H. Singhal, P. Naik, V. Arora, U. Chakravarty, J. Chakera, R. Khan, I. Kulagin, P. Redkin, M. Raghuramaiah, and P. Gupta, "Harmonic generation from indium-rich plasmas," Phys. Rev. A **74**, 063824 (2006).
24. M. Suzuki, M. Baba, R. Ganeev, H. Kuroda, and T. Ozaki, "Anomalous enhancement of a single high-order harmonic by using a laser-ablation tin plume at 47 nm," Opt. Lett. **31**, 3306–3308 (2006).
25. K. J. Schafer, B. Yang, L. F. Dimauro, and K. C. Kulander, "Above threshold ionization beyond the high harmonic cutoff," Phys. Rev. Lett. **70**, 1599–1602 (1993).
26. P. B. Corkum, "Plasma perspective on strong field multiphoton ionization," Phys. Rev. Lett. **71**, 1994–1997 (1993).
27. P. Dietrich, N. H. Burnett, M. Ivanov, and P. B. Corkum, "High-harmonic generation and correlated two-electron multiphoton ionization with elliptically polarized light," Phys. Rev. A **50**, R3585–R3588 (1994).
28. P. Antoine, A. L'Huillier, M. Lewenstein, P. Salières, and B. Carré, "Theory of high-order harmonic generation by an elliptically polarized laser field," Phys. Rev. A **53**, 1725–1745 (1996).
29. P. Salières, B. Carré, L. Le Deroff, F. Grasbon, G. G. Paulus, H. Walther, R. Kopold, W. Becker, D. B. Milošević, A. Sanpera, and M. Lewenstein, "Feynman's path-integral approach for intense-laser-atom interactions," Science **292**, 902–905 (2001)
30. Y. Mairesse, A. de Bohan, L. J. Frasinski, H. Merdji, L. C. Dinu, P. Monchicourt, P. Breger, M. Kovacev, R. Taïeb, B. Carré, H. G. Muller, P. Agostini, and P. Salières, "Attosecond synchronization of high-harmonic soft x-rays," Science **302**, 1540–1543 (2003).
31. V. Véniard, R. Taïeb, and A. Maquet, "Phase dependence of (N+1)-color (N>1) ir-uv photoionization of atoms with higher harmonics," Phys. Rev. A **54**, 721–728 (1996).
32. M. Swoboda, J. Dahlström, T. Ruchon, P. Johnsson, J. Mauritsson, A. L'Huillier, and K. J. Schafer, "Intensity dependence of laser-assisted attosecond photoionization spectra," Laser Phys. **19**, 1591–1599 (2009).
33. R. A. Ganeev, L. B. Elouga Bom, J. C. Kieffer, and T. Ozaki, "Systematic investigation of resonance-induced single-harmonic enhancement in the extreme-ultraviolet range," Phys. Rev. A **75**, 063806 (2007).
34. F. A. Ilkov, J. E. Decker, and S. L. Chin, "Ionization of atoms in the tunnelling regime with experimental evidence using Hg atoms," J. Phys. B. **25**(19), 4005–4020 (1992).
35. E. Constant, D. Garzella, P. Breger, E. Mével, C. Dorrer, C. Le Blanc, F. Salin, and P. Agostini, "Optimizing high harmonic generation in absorbing gases: model and experiment," Phys. Rev. Lett. **82**, 1668–1671 (1999).
36. K. Varjú, Y. Mairesse, B. Carré, M. B. Gaarde, P. Johnsson, S. Kazamias, R. Lopez-Martens, J. Mauritsson, K. J.

#139154 - $15.00 USD Received 3 Dec 2010; revised 17 Jan 2011; accepted 17 Jan 2011; published 10 Feb 2011

Schafer, P. Balcou, A. L'Huillier, and P. Salières, "Frequency chirp of harmonic and attosecond pulses," J. Mod. Opt. **52**, 379–394 (2005).
37. Y. Mairesse, A. de Bohan, L. J. Frasinski, H. Merdji, L. C. Dinu, P. Monchicourt, P. Breger, M. Kovačev, T. Auguste, B. Carré, H. G. Muller, P. Agostini, and P. Salières, "Optimization of attosecond pulse generation," Phys. Rev. Lett. **93**, 163901 (2004).

1. Introduction

High-order harmonic generation (HHG) occurs when an intense short laser pulse is focused into a gas of atoms. It was first shown theoretically [1] and then experimentally [2, 3] that the generated radiation consists of pulses with attosecond duration. This attosecond nature of the harmonic emission, along with its short wavelength, excellent coherence and high brilliance provide a strong motivation for applications, some of which have already been demonstrated. Both trains of attosecond pulses [4–6] and isolated attosecond pulses [7–10] have been used in atomic and molecular spectroscopy and solid-state physics. However, many other applications remain unexplored because of the difficulty to handle and manipulate the harmonics, due partially to the quality of XUV optics, as well as to the low harmonic intensity.

Instead of rare gas atoms, different generating media have been tested in order to increase the conversion efficiency. Recently, attosecond pulses have been successfully generated in molecules. Aligned linear molecules allow a coherent control of the attosecond emission [11], or a tomographic reconstruction of the radiating orbital [12, 13], but unfortunately no real improvement in the efficiency. Due to their high ionization potentials, singly charged ions are interesting candidates since they can withstand higher laser intensity and thus can potentially generate both more intense radiation and higher harmonic orders. Such ions can be produced through ionization of rare gases: HHG in Ar^+ was shown to extend the cutoff to 250 eV [14]. Another possibility is to produce a weakly ionized ablation plasma by focusing a "long" laser pulse on a solid target. The harmonics of a time-delayed short laser pulse are then mainly generated from ions within the underdense plasma plume [15]. Note that overdense plasma is also able to produce high harmonics but through the collective oscillations of the free electrons; this process has been shown recently to result in a train of attosecond pulses [16].

The first experiments in ablation plasma plumes were performed in 1992 by Akiyama et al. [17] and in 1994 by Wahlström et al. [18] in lithium, sodium and potassium media. The highest harmonic achieved was the 27th order for lithium plasma [18]. Recently, this method has re-attracted attention, when Ganeev et al. demonstrated highly efficient (conversion efficiency of 10^{-5}) harmonic generation from silver plasma [19], exceeding conversion efficiencies typically obtained with atomic gases by one order of magnitude [20]. Since then, HHG from more than 15 different target materials has been demonstrated with typical plateau and cutoff features [21], the highest harmonic order being the 101^{st} from a manganese plasma [22]. Different properties of these plasma harmonics have been investigated: The influence of the plasma conditions on the XUV intensity has been studied extensively [15, 23], concluding essentially that a compromise has to be established between the density of singly charged ions mainly responsible for the XUV emission, and that of the free electrons degrading phase matching conditions. Elliptical polarization of the driving laser has been shown to suppress the XUV emission [24], suggesting the "usual" three-step process [25, 26] as its origin, although the drop in the XUV intensity is significantly slower than that known from HHG in neutral gases [27, 28]. However, no temporal characterization has been performed up to now. This is of course a crucial element for the applications of this new source of XUV radiation. It should not be taken for granted that this harmonic emission has a nice attosecond structure. Indeed, the generation in a plasma induces many sources of distortion: the higher electron densities and gradients will affect both the generation through phase matching but also the propagation, and may result in distortions

#139154 - $15.00 USD Received 3 Dec 2010; revised 17 Jan 2011; accepted 17 Jan 2011; published 10 Feb 2011

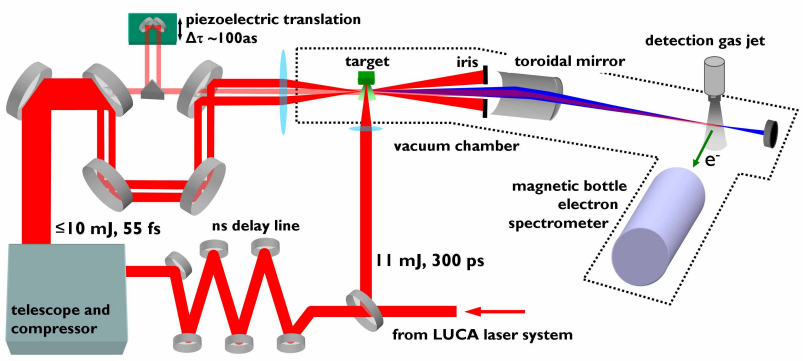

Fig. 1. Experimental set-up for the generation and characterization of the attosecond emission from an ablation plasma.

of both the harmonic spatial phase-front and spectral phase. Furthermore, the temporal characterization itself raises problems, as will be discussed below (probe beam distortions, target deterioration…) In this article, we study the attosecond structure of the harmonic emission from chromium plasma. We first present the experimental setup and discuss the challenges raised by the generation and characterization techniques. We then present the measurements of the amplitude and relative phase of the generated harmonics and discuss the very low positive chirp of the emission. Finally, we reconstruct the attosecond emission combining the 11^{th} to the 19^{th} harmonics and show that it results in pulses that are only 1.05 times the theoretical Fourier transform limit.

2. Experimental Setup and Challenges

In this work, we used the laser facility installed at the Commissariat à l'Energie Atomique (CEA) Saclay. A schematic diagram of the setup is shown in Fig. 1. First, we separated the uncompressed Ti:sapphire laser beam (800 nm, 300 ps) from the "LUCA" laser system into two beams, using a beam splitter. One of these beams (pre-pulse) is loosely focused at normal incidence onto a solid target where it reaches an intensity of $I \sim 10^{10}$ W cm^{-2} and creates the weakly ionized plasma. The other uncompressed beam is first sent through an 80-ns delay line, which includes passage through a compressor. At the exit of the compressor, the 55-fs laser pulse is then further separated into two beams using a mirror with a through hole at the center. The external annular part of the beam (generating beam) is focused (f-number $\approx$ 60) parallel to the target surface into the plasma to generate the high-order harmonics. The round central part of the beam (dressing beam), which is more than two orders of magnitude less intense than the external part, passes through the hole of the mirror and enters a very precise delay line equipped with a piezoelectric translation stage. It is then recombined with the external part of the beam through a second holed mirror. After harmonic generation, an iris blocks the generating beam while the—more collimated—harmonic beam, together with the dressing beam, are refocused by a toroidal mirror into a detection argon jet placed in the source volume of a magnetic bottle electron spectrometer (MBES). The time of flight, and thus the energy, of the electrons produced by photo-ionization of the target gas is measured with an oscilloscope. Note that the medium position after the laser focus—still within the Rayleigh range—together with the spatial filtering of the harmonic beam by the iris made sure that the signal was dominated by the short-trajectory contribution to HHG. However, when scanning the focusing position relative to the medium or opening somewhat the mentioned iris, we never

#139154 - $15.00 USD Received 3 Dec 2010; revised 17 Jan 2011; accepted 17 Jan 2011; published 10 Feb 2011

observed shoulders or broadening of the harmonic peaks as a clear spectral signature of a long-trajectory contribution [29].

A crucial element in this setup turned out to be the 80-ns delay line. The passage through the compressor imposes already a delay of ≈ 20 ns, leaving 60 ns, corresponding to 18 m of propagation, to be added. Note that the precise length is not very important — as long as the delay between plasma creation and HHG is > 50 ns, the ablation plasma conditions should be stable [23]. In this campaign, the delay line was a simple four-time-passage through 4.5 m of air. Although the laser pulse is still rather long in this delay line and its peak power thus limited, the long propagation through air introduced (mainly spatial) laser beam distortions. This deteriorated spatial beam quality limited the focal intensity in the HHG chamber to less than 2×10^{14} W cm^{-2} (as opposed to $> 10^{15}$ W cm^{-2} used in past works). This effective intensity at focus was estimated by measuring the attochirp of the harmonic emission from an argon gas jet in the same experimental conditions [30]. This limitation to an intensity a factor 2.5 to 5 below what is typically used for HHG in ablation plasma plumes may be the reason for the low level of XUV signal in our experiments with all targets we have used. The rather poor phase matching in the HHG medium due to the strong wavefront distortions of the driving laser beam may be another reason. Using a tighter focusing of the generating beam was not easily achievable without risking making necessary significant modifications to the optical setup for the temporal characterization, which had proven very reliable in earlier measurements [6, 11, 13]. We therefore preferred to leave our well-proven optical setup unchanged during the limited time of this measurement run.

The characterization of the plasma attosecond emission was performed using the RABITT technique (Reconstruction of Attosecond Beating by Interference of Two-photon Transitions) [2]. The measurement of the harmonic spectral amplitude and phase allows a direct access to the attosecond structure through a Fourier transform. The amplitude of each harmonic is easily given by the amplitude of the main photoelectron lines corrected for the ionization cross section. The relative phase between neighboring harmonic orders is accessed through two-photon XUV+IR ionization of the target gas. When the dressing beam is superimposed on the XUV beam in the argon gas, sidebands appear in the photoelectron spectrum between the main lines. They correspond to two-photon transitions: absorption of a harmonic photon $q\omega_0$ accompanied by either absorption or stimulated emission of a laser photon ω_0. Since two coherent quantum paths lead to the same sideband, interferences occur which result in an oscillation of the sideband amplitude as the delay τ between the IR and harmonic field is scanned with sub-IR-laser-cycle resolution [2, 31]. The phase of the oscillation is the phase difference between the two interfering channels. It is determined by the phase difference $\varphi_q - \varphi_{q+2}$ between consecutive harmonics (phase locking) and by the difference, $\Delta\phi^{\mathrm{at}}$, of the two-photon transition dipole phases. For example, if we consider the (q+1)$^{\mathrm{th}}$ sideband between the q^{th} and the $(q+2)^{\mathrm{th}}$ harmonic order, the signal intensity is:

$$S_{q+1}(\tau) = \alpha + \beta\cos\left(2\omega_0\tau + \varphi_q - \varphi_{q+2} + \Delta\phi^{\mathrm{at}}\right), \tag{1}$$

where α and β are positive real valued constants. The term $\Delta\phi^{\mathrm{at}}$, characteristic of the target gas argon, is small and can be calculated [2, 31]. The phase difference $\varphi_q - \varphi_{q+2}$ between two consecutive harmonics can then be extracted, readily giving the group delay, also called emission time $t_{\mathrm{e}} = \partial\varphi/\partial\omega|_{q+1} \approx -(\varphi_q - \varphi_{q+2})/2\omega_0$.

The RABITT technique, being based on the delay between the XUV and IR dressing beams, requires the (undelayed) intense IR generating beam to be blocked efficiently before the target gas. If this is not the case, it may interfere with the dressing beam and—if intense enough—even produce above-threshold ionization of the target gas, leading to distortions in the RABITT measurements. This condition imposed a minimum distance of the generating beam to the target

#139154 - $15.00 USD Received 3 Dec 2010; revised 17 Jan 2011; accepted 17 Jan 2011; published 10 Feb 2011

surface: we had to avoid the large gradient of the free electron density close to this surface, since it refracts a significant part of the generating beam, which is then no longer fully blocked by the iris before the target gas. To minimize this effect, we generated harmonics in the plasma plume at a distance of 200–300 μm from the target surface. This made sure that the refracted IR light from the generating beam did not generate sidebands on its own, i.e. its intensity was considerably weaker than that of the IR dressing beam in the MBES interaction volume. Due to the rapid drop of plasma density with the distance from the target surface, this resulted in a decrease by a factor of ~ 2 in the generated XUV energy as compared to a focusing closer to the surface. Note that the smaller and more homogeneous electron density obtained at this distance also results in less phase-front distortions of the IR dressing beam, as needed by the RABITT technique. Indeed, the phase relationship between the XUV and dressing beams must be homogeneous in the detection volume, otherwise the sideband oscillations are blurred. The phase-front quality of both beams was a major concern when the experiment was planned and could have been a reason of failure.

The low level of harmonic signal resulted in very weak sideband amplitudes (they must be kept at least a factor 3 smaller than the main lines in order to be in the linear—single IR photon—regime [32]). This could hardly be dealt with by averaging over more laser shots per photoelectron spectrum, due to the deterioration of the solid target: it was not moved during data acquisition, i.e. the picosecond pre-pulse hit the surface always at the same spot. Very little material is actually ablated per laser shot and most targets could easily withstand $\sim 10^3$ shots without any degradation of the generated XUV signal. For a RABITT measurement, however, we typically use 10^4 laser shots (100 delay steps and averaging 100 shots per spectrum), so there was really no margin left to increase the averaging. On the contrary, the IR-XUV delay scans had to be kept rather short and were accompanied by a gradual decline in signal during the scans.

Attosecond pulse measurements proved to be extremely hard and we encountered big difficulties in observing clean $2\omega_0$-oscillations of the sidebands. The mechanical stability of the setup was absolutely sufficient as proven by: i) clear $2\omega_0$-oscillations in the RABITT scans with harmonics generated in argon during the same measurement campaign; ii) a very well resolved ω_0-modulation of the total signal in most scans with ablation plasma harmonics (originating from the interference of the probe and generating IR beams in the generating medium). The reasons for our difficulties were threefold: i) the rather low spatial beam quality and energy stability of the laser after the delay line, leading to noise and a decreased contrast of the $2\omega_0$-oscillations in the RABITT signal; (ii) additional distortions of the IR dressing beam during propagation in the plasma medium, which may further reduce this contrast; (iii) the requirement that the sidebands be kept rather weak, together with the low XUV signal and the limited acquisition times imposed by sample degradation, that resulted in difficult conditions for RABITT measurements.

3. Experimental Results and Discussion

Despite all the difficulties mentioned above, we succeeded in measuring series of RABITT scans in chromium plasma with significant and reproducible $2\omega_0$-oscillations of the sideband amplitudes. Let us first consider the generated harmonic spectrum, shown in Fig. 2, obtained from the photoelectron spectrum measured without the dressing beam.

This harmonic spectrum differs considerably from those observed in other works. Past results using 35 fs Ti:sapphire laser pulses have demonstrated chromium harmonic spectra with cut-off at the 35^{th} order, with strong intensity enhancement of the 29^{th} harmonic [33]. In contrast, the spectrum in Fig. 2 has a cut-off at the 19^{th} order. This is the result of the relatively low generating laser intensity due to the spatial beam distortion induced by the delay line, as explained in

#139154 - $15.00 USD Received 3 Dec 2010; revised 17 Jan 2011; accepted 17 Jan 2011; published 10 Feb 2011

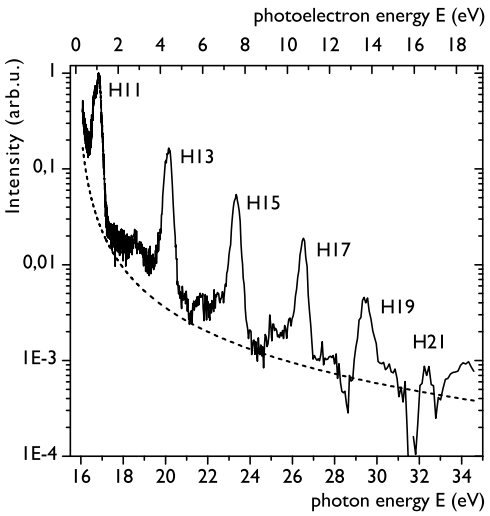

Fig. 2. Harmonic spectrum obtained from the chromium plasma. The spectrum shows five consecutive harmonic orders, from the 11$^{\text{th}}$ to the 19$^{\text{th}}$ harmonic. The dashed line indicates the noise floor of the MBES signal.

the previous section. An intensity just below $2\times10^{14}\,\mathrm{W\,cm^{-2}}$ saturates harmonic generation in Cr^{+} ($I_p = 16.5\,\mathrm{eV}$) but may be too low to generate efficiently in Cr^{2+} ($I_p = 31\,\mathrm{eV}$). This is due to the barrier-suppression intensity, $I_{\mathrm{BSI}}[\mathrm{Wcm^{-2}}] = 4\times10^{9}(I_p[\mathrm{eV}])^4/Z^2$, being $7\times10^{13}\,\mathrm{W\,cm^{-2}}$ for Cr^{+} ions and $4\times10^{14}\,\mathrm{W\,cm^{-2}}$ for Cr^{2+} ions [34]. Here, Z is the effective charge of the screened nuclei, i.e. $Z=2$ for ionization of Cr^{+} and $Z=3$ for Cr^{2+}. The saturation intensity for Cr^{+} ions together with their ionization potential give a classical cut-off position [25, 26] at the 19$^{\text{th}}$ harmonic, which is in good agreement with the experimental observation. For Cr^{2+} ions and an intensity of $2\times10^{14}\,\mathrm{W\,cm^{-2}}$, a classical cut-off at the 43$^{\text{rd}}$ harmonic is expected. We thus conclude that we generate harmonics mainly in the rising edge of the pump pulse in Cr^{+} ions without a significant contribution from Cr^{2+} ions, in contrast to previous experiments. Note that the laser defocusing induced by the electron density gradients in the plasma may also result in a reduced effective peak intensity.

Another important difference is that the efficiency drops exponentially with harmonic order in the current work, whereas a plateau in the spectra was observed in past works. The phase mismatch due to free electrons in the plasma cannot explain the observed rapid drop of the spectral intensity. Assuming an emission limited by phase mismatch, the spectral intensity varies as [35]:

$$I_q \propto L_{\mathrm{coh}}^2[1-\cos(\pi L_{\mathrm{med}}/L_{\mathrm{coh}})], \tag{2}$$

where L_{med} is the medium length and $L_{\mathrm{coh}} = \pi/\Delta k_{\mathrm{e}}$ is the coherence length resulting from the mismatch between the harmonic and driving polarization wave vectors $\Delta k_{\mathrm{e}} = k_q^{\mathrm{e}} - qk_1^{\mathrm{e}}$. The wavevector of the q$^{\text{th}}$ harmonic can be written as:

$$k^{\mathrm{e}}{}_q = \frac{1}{c}\left(q^2{\omega_0}^2 - {\omega_{\mathrm{p}}}^2\right)^{1/2} \approx \frac{q\omega_0}{c}\left(1-\frac{{\omega_{\mathrm{p}}}^2}{2q^2{\omega_0}^2}\right), \qquad \text{with} \quad {\omega_{\mathrm{p}}}^2 = \frac{n_{\mathrm{e}}e^2}{m_{\mathrm{e}}\varepsilon_0}, \tag{3}$$

where ω_{p} is the plasma frequency, m_{e} and e are the electron mass and charge, respectively, c is the vacuum light velocity, and n_{e} is the plasma electron density. We estimate the free electron density to be $1\times10^{17}\,\mathrm{cm^{-3}}$ [21], leading to coherence lengths of $L_{\mathrm{coh}} = 1.25\,\mathrm{mm}$ for the 11$^{\text{th}}$ harmonic, and 0.73 mm for the 19$^{\text{th}}$ harmonic. For our observed spectral range, L_{coh} is thus

#139154 - $15.00 USD Received 3 Dec 2010; revised 17 Jan 2011; accepted 17 Jan 2011; published 10 Feb 2011

always longer than the typical length of our plasma medium of 0.6 mm and the phase matching situation should be quite good. Equation 2 then only predicts the spectral intensity to drop by a factor $\sim$ 2–3 from the 11$^{\text{th}}$ to the 19$^{\text{th}}$ harmonic, whereas in the experiment (cp. Fig. 2), it drops by more than two orders of magnitude. This can only be attributed to the cut-off in the single-ion response (Cr^+ high harmonic spectrum), in agreement with our above conclusion.

Let us now turn to the oscillations of the sideband amplitudes obtained when superposing the dressing beam and varying the delay. The Fourier-transformed sideband-signals of one of the RABITT scans are shown in Fig. 3. As usually performed in the case of rare gases, the sideband signals have been normalized for each delay to the total photoelectron signal before Fourier transforming. This procedure removes the ω_0-oscillations resulting from the modulation of the harmonic emission due to the interference of the generating and dressing beams in the generating medium. Clearly, the remaining ω_0-component in Fig. 3 is exceptionally strong; it is due to the above-mentioned strong scattering of IR light from the generating beam into the MBES interaction volume. The $2\omega_0$-peaks are much less pronounced than usually obtained in rare gases, but they are nonetheless clearly distinguishable from the surrounding noise. The reproducibility of the measured emission times finally gives confidence in this data.

Figure 4(a) shows the emission times t_e extracted from the sideband oscillations. The results show a very low positive group delay dispersion (GDD) of 20 as between two successive harmonics, corresponding to a GDD of 4200 as^2. This corresponds in the time domain to a chirp of the attosecond emission, also called attochirp. Such a chirp has been intensively studied in rare gases and small molecules: it is intrinsic to the HHG process and corresponds to the drift of the recombination times associated with the different electron trajectories involved in the harmonic emission [30, 36]. However, for the generating intensity used here, the GDD should be more than two times larger for harmonics in the plateau region [30]. Assuming an effective generating intensity equal to the saturation intensity of Cr^+ ions, the GDD should even be 6 times as large since the GDD is inversely proportional to the intensity. A possible cause for the small GDD could be the free electron density in the plasma medium that induces a dispersion of opposite sign to the intrinsic GDD. From Eq. 3, with $q\omega_0 = \omega$, we find the group velocity dispersion $\partial^2 k/\partial\omega^2 = c^{-1}\left[(\omega^2-{\omega_p}^2)^{-1/2} - \omega^2(\omega^2-{\omega_p}^2)^{-3/2}\right] \approx -{\omega_p}^2 c^{-1}\omega^{-3}$ added by propagation through a free electron gas with a density $n_e = 1\times10^{17}\,\text{cm}^{-3}$. It amounts to $-60\,\text{as}^2\,\text{mm}^{-1}$ for the 11$^{\text{th}}$ harmonic and $-12\,\text{as}^2\,\text{mm}^{-1}$ for the 19$^{\text{th}}$ harmonic, which is far too small to compensate for the intrinsic GDD. The only way to reconcile the measured GDD value with the Strong Field Approximation theory and the previous measurements in atomic gases is to consider that the measured harmonics are in the cutoff region of the ion spectrum, where the emission times saturate and the chirp tends to vanish [37].

From the phases φ_q, obtained by integrating the emission times, and the amplitudes A_q of the harmonic orders, we can reconstruct the temporal intensity profile $I(t)$ according to:

$$I(t) = \left|\sum_q A_q \exp[-\mathrm{i}q\omega_0 t + \mathrm{i}\varphi_q]\right|^2 . \tag{4}$$

The result for the measured five harmonic orders $q = 11$ to 19 is shown in Fig. 4(b). The reconstructed temporal profile of the harmonic emission forms an attosecond pulse train, with each pulse of 300 as duration (full width at half maximum). If we assume all 5 harmonics to be in phase, we obtain the shortest pulses possible, i.e. the Fourier-transform limited pulses. The corresponding duration is $\tau_{FL} = 285\,\text{as}$. The measured duration of 300 as is thus only 1.05 times the Fourier transform limited duration. Note that despite their low relative spectral intensity (see Fig. 2), the highest harmonic orders give an important contribution to the reconstructed pulse train. For example, when excluding harmonic 19 from the superposition, the pulse width increases to 360 as.

#139154 - $15.00 USD Received 3 Dec 2010; revised 17 Jan 2011; accepted 17 Jan 2011; published 10 Feb 2011

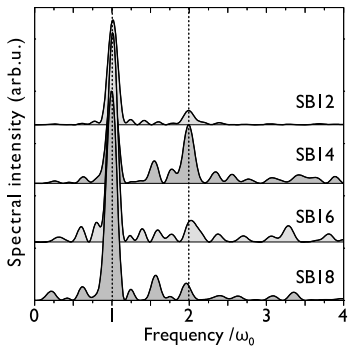

Fig. 3. Squared Fourier-transforms of the four evaluated sideband signals.

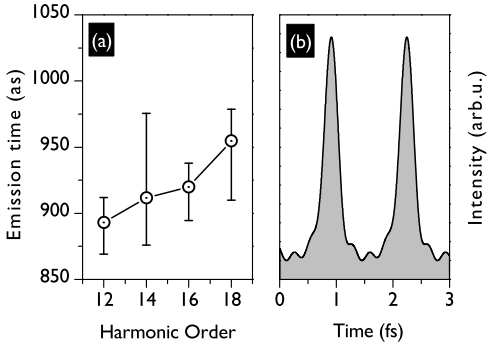

Fig. 4. Emission times (a) and temporal profile (b) corresponding to the 11^{th} to the 19^{th} harmonic orders. The emission times are an average over two RABBIT scans made under equal conditions and the error bars show the range covered by the error bars of these individual scans, which are themselves obtained as the standard deviation of the phase of the Fourier transformed sidebands within the FWHM of the $2\omega_0$ peak.

4. Conclusion

In this article, we have first discussed the challenges raised by the characterization of the attosecond emission of ablation plasmas. Despite the many difficulties, we were able to measure the spectral phase of the harmonic emission from chromium plasma. It exhibits an unexpectedly low GDD that can be explained by the fact that the measured harmonic orders belong to the cutoff region of the Cr^+ HHG spectrum. The reconstructed temporal profile corresponding to five consecutive harmonics is a train of pulses, with each pulse having an average duration of 300 as. This corresponds to 1.05 times the Fourier transform limit. Considering the potentially very high conversion efficiency when using higher generating intensity, these results indicate that plasma harmonics could become a source for generating intense attosecond pulses. Indeed, our measurements show that the generation and propagation in the plasma do not significantly affect the GDD resulting from the single-ion response. Generation at the saturation intensity of the Cr^{2+} ions, i.e. at 4×10^{14} W cm^{-2}, should both extend the plateau and result in a plateau GDD of 5300 as^2, low enough to generate intense 110-as pulses if 12 harmonic orders are selected.

Acknowledgements

L.B.E.B. and T.O. would like to acknowledge financial support from the Ministère du Développement économique, de l'Innovation et de l'Exportation Québec (MDEIE), and the Natural Sciences and Engineering Research Council of Canada (NSERC). S.H. acknowledges funding by the Austrian Science Fund (FWF) grants 21463-N22 and M1260-N16. P.S. acknowledges financial support from the EU-FP7-ATTOFEL and the ANR-09-BLAN-0031-01 Attowave program.

#139154 - $15.00 USD Received 3 Dec 2010; revised 17 Jan 2011; accepted 17 Jan 2011; published 10 Feb 2011